Luminescent Materials

DOI: 10.1002/anie.200804005

Recent Developments in the Field of Inorganic Phosphors**

*Henning A. Höppe**

displays · luminescence · materials science · phosphors · rare earths

Because fossil fuels are becoming scarce and because of the expected climate change, our standard of living can only be maintained by a significant increase in energy efficiency. Large amounts of energy are consumed for lighting and during operation of displays. Thus, the targets are the development of economical light sources like white-light-emitting diodes and display panels with enhanced efficiency. Solar energy is converted into electricity by solar cells, and their efficiency must be improved considerably. A possible contribution might be delivered by phosphors which allow the conversion of thermal radiation into electrical energy. Although the target of energy efficiency is very important, we must not overlook that medical imaging diagnostic methods require efficient and sensitive detectors. For the solution of these central questions, inorganic solid-state materials doped with rare-earth ions are very promising and are therefore in the focus of current research activities.

1. Introduction

The driving forces of the recent developments covered in this Minireview are climate change, energy saving, and energy efficiency. There is even political support for alternative solutions in the form of light-bulb bans and climate-saving emissions targets. Moreover, medical diagnostics is interested in more sensitive detection materials to make novel 3D imaging techniques more gentle for patients.

The first review in *Angewandte Chemie* on phosphors for lighting and display applications[1] appeared about ten years ago. At that time, the improvements over the previous thirty years had yielded phosphors thought to be working on the edge of the physically possible. Further improvements of properties such as quantum efficiency or spectral dispersion were not expected in the near future. Furthermore, it seemed improbable that new materials with significantly better properties would be found.

With respect to low-pressure mercury phosphorescent tubes, this assessment is probably correct. But there have been fundamental improvements and novel developments in the area of white LEDs (light-emitting diodes; Section 2), advances in the improvement of plasma displays (Section 3), significant progress with respect to scintillators (Section 4), the synthesis of nanostructured phosphors (Section 5), and improvements of upconversion phosphors (Section 7). Some progress has also been made with quantum-cutting phosphors (Section 6). The discussion of the advances on white LEDs must be limited to a selection owing to the extraordinarily rapid progress in this field. Recent developments of luminescent complexes[2] and organic phosphors for OLEDs[3] as well as in my opinion less prominent topics such as Ce^{IV} compounds as UV absorbers in sunglasses or sunscreen[4] were not considered for this Minireview.

For explanations of important terms concerning phosphors, such as quantum efficiency, color coordinates, and color temperature, I refer the reader to the earlier Review.[1]

[*] Dr. H. A. Höppe
Institut für Anorganische und Analytische Chemie
Albert-Ludwigs-Universität Freiburg
Albertstrasse 21, 79104 Freiburg (Germany)
E-mail: henning.hoeppe@ac.uni-freiburg.de

[**] This work was supported by the Fonds der Chemischen Industrie (Liebig-Habilitationsstipendium). The author thanks the referees for helpful comments.

2. Light-Emitting Diodes: Efficient Light Source of the Future

2.1. Rare-Earth Ions with f→d Transitions

A good phosphor should absorb the excitation energy and emit light afterwards as efficiently as possible. In other words, the quantum efficiency[5] should be maximized. The elapsed time between excitation and emission should be very short to avoid afterglow. Especially in applications such as displays, detectors (scintillators), and traffic lights, an afterglow would be disadvantageous. To achieve this goal, transitions with high transition probabilities and short lifetimes are needed. These criteria are best met by rare-earth ions. Their 4f states only weakly interact with the host lattice, and therefore the energy differences are nearly constant. Moreover, they show a low tendency for radiationless relaxations. The transitions should also be parity-allowed, and therefore the efficiency of ions that show 4f→5d transitions is normally very high. For excitation with UV or blue light this is only the case for Ce^{3+} and Eu^{2+}; for excitation in the vacuum UV (VUV) radiation, this applies for almost every rare-earth ion.

An overview of experimental data was collected by Dorenbos.[6,7] Exact predictions of excitation and emission wavelengths of doped host lattices are very complicated owing to the complexity of numerous variables and cannot replace the synthesis of phase-pure doped host lattices.

The investigation of phosphors excited in the vacuum UV requires knowledge about the energetic position of f levels in this region. After the systematic extension of the Dieke diagram[8,9] up to VUV excitations, the emitting states were also identified.[10]

2.2. White-Light-Emitting Diodes

Since Nakamura solved the problem of p doping[131] and enabled technological access to blue LEDs,[11] their further development has proceeded at a rapid pace. Their efficiency has improved continually, and their emission wavelength can be tuned to longer wavelengths by cocrystallization with InN and towards shorter wavelengths by cocrystallization with AlN. This approach leads to improvements of white LEDs and the need for suitable phosphors.

Henning Höppe was born in Nuremburg (Germany) in 1972. He studied Chemistry at the University of Bayreuth and obtained his Ph.D. from the Ludwig-Maximilians-Universität Munich under the supervision of Prof. Dr. W. Schnick. From 2003 to 2004 he worked as a postdoctoral researcher with Prof. M. L. H. Green FRS at the University of Oxford. Since autumn 2004 he has been a young research group leader at the Albert-Ludwigs-Universität in Freiburg im Breisgau. His work in the area of new optic functional materials is supported by a Liebig grant of the Fonds der Chemischen Industrie.

White LEDs can save approximately 70% of the energy used for incandescent light bulbs[12] and do not need the hazardous mercury commonly used in luminescent tubes. Compared with these, which require excitation at 254 nm, LEDs also save energy by using a longer excitation wavelength of 330 to 450 nm. Thus the energy difference between emitted light and excitation source is smaller in white LEDs. OLEDs will not be discussed in detail in this article, but it should be noted that, owing to their materials properties, they exhibit much shorter lifetimes and do not achieve as high of light yields as inorganic LEDs. The organic materials used in OLEDs are not sufficiently stable towards radiation. The future of OLEDs lies in their potential for large-scale and transparent lighting applications[3] like luminescent curtains, walls, and displays in mobile phones, for which long lifetimes are of minor importance.

There are three different technical approaches for the realization of inorganic white LEDs.[13] The first successful device combined a blue LED covered with a classical yellow phosphor, such as yttrium aluminum garnet $Y_3Al_5O_{12}$ doped with Ce^{3+} (YAG:Ce^{3+}).[14] These LEDs have been broadly used as simple long-life white-light sources in traffic lights, cycle lamps, car headlights, outdoor lighting, flashlights, or marking lamps in tunnels. The obtained light looks bluish-cold owing to its high color temperature.[15]

More sophisticated applications like indoor lighting require warm-white light and an excellent color rendering. The white light should contain red wavelength parts and thus exhibit a lower color temperature. These targets are met by combination of a blue (Ga,In)N LED with two phosphors emitting red and green light.

In the third approach suitable phosphors for (Ga,Al)N UV LEDs are developed. These are covered with three different phosphors, which emit red, green, and blue. The advantage of these white LEDs is that they enable variation of three broad-band emitters, giving access to a larger color area in the CIE diagram (Figure 1) and better color rendering. Thus, the light source becomes more similar to sunlight.

The light emitted by a blue or UV LED is considerably more intense than that generated in a mercury plasma.[16] This situation demands a special stability of the phosphors towards thermal fluorescence quenching and of the host lattice

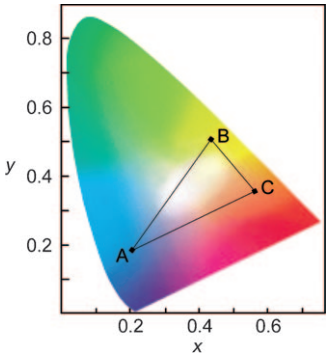

Figure 1. Color diagram of the CIE (CIE = Commission Internationale d'Eclairage); by mixing of the three emissions A, B, and C defined by their color coordinates, all white shades within the triangle are accessible.

towards radiation. Moreover, the phosphors developed until the 1990s were optimized for the excitation wavelength of mercury plasma (254 nm), while the excitation in LEDs occurs between 330 and 450 nm. To avoid energy loss, the optimum excitation wavelength has to be adjusted to the emission of the LED. In this case, broad-band excitation is advantageous, as the emission wavelength of commercial blue and UV LEDs varies for technological reasons.

2.3. Three-Color LEDs

The realization of an all-nitride white LED[17] follows the second presented approach. In this white LED, only nitrides, a highly interesting class of compounds in this context owing to their stronger nephelauxetic effect compared to oxides, are used.[18] A blue-emitting GaInN chip is covered with the orange-luminescent nitridosilicate $Sr_2Si_5N_8:Eu^{2+}$[19] and the green-fluorescing $SrSi_2O_2N_2:Eu^{2+}$ (other examples: $CaSi_2O_2N_2$[20], $EuSi_2O_2N_2$[21]). Figure 2 shows the setup of this

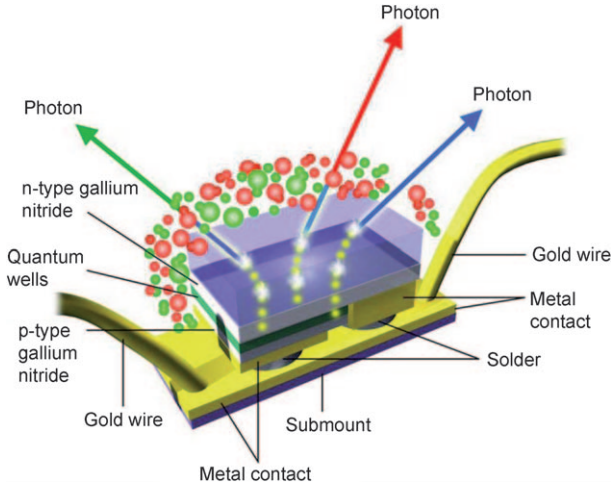

Figure 2. Schematic depiction of a warm-white-emitting diode[17] based on a blue LED coated with a green and a red phosphor.

LED. Figure 3 presents the excitation and emission spectra of phosphors used for white LEDs. The color rendering index[1] of this warm-white LED is around 90, its color temperature is 3200 K. Fine adjustment of the red emission wavelength of $Sr_2Si_5N_8:Eu^{2+}$ is achieved by partial substitution of Sr by Ca.[19,22] As a consequence, the crystal-field splitting of the d levels of the doped Eu^{2+} ions changes. Secondly, the covalence of the bonds from Eu^{2+} to the coordinating atoms can be varied systematically. Another white LED with a significantly higher color temperature of 5200 K was made using a blue LED chip in combination with the previously mentioned $SrSi_2O_2N_2:Eu^{2+}$ and red-emitting $CaSiN_2:Eu^{2+}$. Its color rendering index amounts to 90.5.[23] Thus, small changes of the phosphor mixture allow the realization of almost every desired color temperature.

An interesting green-emitting phosphor is the europium-doped nitridosilicate $BaSi_3N_5$, which shows a broad-band emission peak at 549 nm.[24] Other promising red phosphors

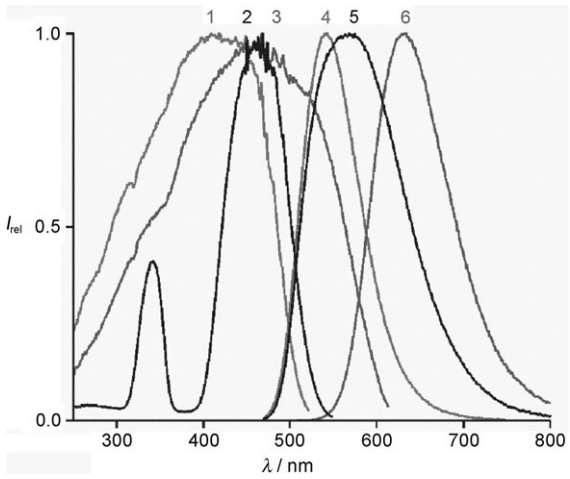

Figure 3. Excitation and emission spectra of phosphors for white LEDs; $SrSi_2O_2N_2:Eu^{2+}$ (excitation: 1, emission: 4), $YAG:Ce^{3+}$ (excitation: 2, emission: 5), $Sr_2Si_5N_8:Eu^{2+}$ (excitation: 3, emission: 6).[17]

are $Ca_2ZnSi_2O_7:Eu^{2+}$, which absorbs efficiently at 460 nm and emits at 600 nm,[25] as well as $SrS:Eu^{2+}$.[26,27] As a possible green component, the thiogallate $SrGa_2S_4:Eu^{2+}$[26,28,29] was considered. Both SrS and $SrGa_2S_4$, however, suffer from thermal instability and are easily hydrolyzed.[30,31] The thiogallate $ZnGa_2S_4:Eu^{2+}$, which emits at 536 nm, is also interesting. In this case, the Eu^{2+} ions are situated in octahedral voids instead of on the original zinc positions.[32] The reason for this arrangement is that Zn^{2+} ions are much smaller than Eu^{2+} ions. Consequently, the Eu^{2+} ions occupy larger voids in the crystal structure.

New approaches for green phosphors are exemplified by the first investigations on terbium dicyanamides[33] and Eu^{2+}-doped thiocyanates with main emissions in the green at 508 ($Sr(SCN)_2$[34]) and 511 nm ($Ba(SCN)_2$). Unfortunately, these emissions can only be observed below 220 (Sr) and 280 K (Ba).[35]

Meanwhile, UV LEDs on the basis of (Al,Ga)N are technologically available, allowing emission wavelengths down to 330 nm.[36] Such LEDs in combination with suitable phosphors should give access to a larger color area in the CIE color diagram (Figure 1) compared with the white LEDs discussed in Section 2.2. A basic technical problem results from the fact that in the case of a UV LED, three different phosphors have to be arranged. A solution is offered by phosphors which emit at least two wavelengths simultaneously. One current example is the two-color phosphor α-$Sr(PO_3)_2:Eu^{2+},Mn^{2+}$, which emits white light under UV excitation.[37] The blue luminescence of Eu^{2+} combined with orange-emitting Mn^{2+} gives a white emission. In principle, Mn^{2+} is a very bad emitting ion because all transitions in a d^5 high-spin system are forbidden by parity and spin selection rules. The low site symmetry in α-$Sr(PO_3)_2$[38] allows for mixing with states of different parity, leading to higher transition probabilities. Furthermore, the highly symmetric arrangement of the Sr^{2+} ions favors a pairing of the doped defects, making the energy transfer from Eu^{2+} to Mn^{2+} significantly more efficient.[39] Consequently, Eu^{2+} can act as sensitizer and transfer part of its excitation energy onto

neighboring Mn^{2+} ions. Further examples are the similarly doped $CaAl_2Si_2O_8$[40] and $Ba_3MgSi_2O_8$.[41] For these species, a pairing of the doped ions is not likely. Other phosphors for white-light-emitting diodes based on UV LEDs might be the doped thiosilicates $Ca_2SiS_4:Eu^{2+}$ (red), $BaSi_2S_5:Eu^{2+}$ (green), and $Ba_2SiS_4:Ce^{3+}$ (blue),[42] which unfortunately suffer from instability towards moisture.

3. Phosphors for Plasma Displays

In plasma display panels (PDP), individual light points are generated by igniting a low-pressure inert-gas plasma (Xe, Xe/Ne) approximately every 5 ms. The resulting VUV radiation[43] excites phosphors to emit the three basic colors. Currently, the well-known phosphors BAM ($BaMgAl_{10}O_{17}:Eu^{2+}$, blue), ZSM ($Zn_2SiO_4:Mn^{2+}$, green), and YGB ($(Y,Gd)BO_3:Eu^{3+}$, red) are employed;[1] some of these materials are also commonly used in fluorescent tubes. All of these phosphors can be excited very well in the VUV region, but with enduring operation emission intensity decreases significantly, especially for $BaMgAl_{10}O_{17}:Eu^{2+}$. After 30 h continuous irradiation in the VUV, the luminescence of BAM is reduced by approximately 25% owing to thermal decomposition and because the host lattice is sensitive to the radiation.[44]

3.1. The Blue Color Point

Structures crystallizing isotypically to β-alumina, such as BAM, often have a large number of defects.[45–48] Moreover, at higher temperatures the oxidation of Eu^{2+} to Eu^{3+} on the surface is observed.[49,50] In the case of BAM, there are no indications for an analogous oxidation caused by radiation, but structural changes in the host lattice are likely.[50] This situation is suggested by the quickly decreasing stability of BAM under radiation with wavelengths below 175 nm, which is equal to the band gap of the host lattice.[51] The resistance to radiation and the thermal stability is improved by coating the phosphor particles with $AlPO_4$, Al_2O_3, or SiO_2.[44] The emission power of BAM can be increased by codoping with Nd^{3+} or Er^{3+}.[52] This approach yields defined anion defects, which shift the excitation band from 166 to 172 nm. Thus the modified BAM absorbs the main emission of the Xe plasma more efficiently.

$LaPO_4$ doped with Tm^{3+} (LPTM) is very promising as an alternative to BAM. Its band gap is 8 eV, and it crystallizes in the monoclinic crystal system isotypically with monazite. Owing to the low symmetry around the cation, $LaPO_4$ is very well suited as a host material. The main emission at 452 nm is accompanied by some undesirable emissions in the near UV region. These emissions diminish the brilliance of LPTM. Compared with BAM, it is much more stable towards high temperatures and more resistant towards radiation, especially below 200 nm.[53] If used in a blend with 50% BAM, the undesirable emissions in the UV are absorbed. The emission of the mixtures is very brilliant, and BAM simultaneously suffers less damage from radiation.

3.2. The Red Color Point

The currently used red phosphor $(Y,Gd)BO_3:Eu^{3+}$ (YGB) crystallizes in the vaterite lattice. YGB exhibits a high quantum efficiency and is very stable towards heat and radiation,[54,55] in contrast to BAM. However, YGB shows an additional orange emission at 592 nm which is assigned to the $^5D_0 \rightarrow {}^7F_1$ transition in Eu^{3+}. This emission reduces the color purity of YGB,[56–58] which has its main red emission at 611 nm ($^5D_0 \rightarrow {}^7F_2$). Color filters suppress the additional emission, but this approach diminishes the brilliance. $(Y,Gd)_2O_3:Eu^{3+}$ is more brilliant, but it is not stable under radiation in the VUV.[44] By doping YGB with Lu^{3+} as in $(Y,Gd,Lu)BO_3:Eu^{3+}$ the brilliance might be enhanced by approximately a fifth.[59] Apparently the local symmetry around the Eu^{3+} ion is changed, thus changing the emission behavior.

An alternative might be the use of nanoscale YGB particles in which the local symmetry around the Eu^{3+} ion is distorted by defects, thus favoring the desired $^5D_0 \rightarrow {}^7F_2$ transition.[60] The phase-pure synthesis of these nanoparticles is still a difficult task,[61] and there is still great interest in the discovery of better red phosphors.

3.3. The Green Color Point

Zn_2SiO_4 (ZSM) doped with Mn^{2+} is more stable toward radiation than BAM, but owing to its sensibility toward ionic bombardment, it also decomposes during operation.[44] Moreover, the decay time (15 ms) of the green transition $^4T_1 \rightarrow {}^6A_1$ in Mn^{2+} is too long (compared with 10 ms for Eu^{3+} in YGB)[62] and thus is disadvantageous for the application in PDPs. The emission of ZSM decays faster after codoping with Ba^{2+} or Gd^{3+}, but the efficiency of the phosphor decreases simultaneously by 20 or 14%, respectively.[63] If this phosphor is not synthesized by a solid-state reaction but by spray pyrolysis with subsequent tempering under reducing conditions, the quantum efficiency is higher than that of common ZSM.[64] The germanate $Li_2ZnGe_3O_8$ doped with Mn^{2+} tops ZSM in terms of brilliance and stability towards the exciting plasma but looses versus ZSM owing to its worse heat stability.[44]

The emission of green phosphors based on doping with Tb^{3+}, such as $YBO_3:Tb^{3+}$, decays faster than 10 ms. Undesirable blue emissions around 490 nm ($^5D_3 \rightarrow {}^7F_j$; $j = 1 \ldots 6$) decrease the color purity demanded by the manufacturers[56–58] and therefore the quality of this phosphor. To suppress the undesired emission a higher Tb concentration is used, which causes an increase in intensity of the green transitions $^5D_3 \rightarrow {}^7F_j$ by reducing the blue emission. Furthermore, the use of phosphor blends with ZSM was suggested.[65]

In summary there is still a need for new phosphors which show long-term stability under the provided conditions and simultaneously exhibit short decay times and high efficiencies.

4. Scintillation Materials

Scintillation materials are used in detectors of highly energetic radiation (X-rays, γ radiation, etc.). In a scintillation

crystal, the host lattice absorbs the ionizing radiation by forming electron–hole pairs (excitons[73]). The activation energy is finally transferred onto doped activator ions such as Ce^{3+}, which relax to their ground state under emission of light. Commonly used X-ray detectors are $Gd_2O_2S:Tb^{3+}$[66] or $BaFBr_{1-x}I_x:Eu^{2+}$ ($x \leq 0.2$),[67] $CsI:Tl^+$,[68] and $CaWO_4$.[69] New medical applications, such as the imaging techniques positron emission tomography (PET), computer tomography (CT), and single-photon computer tomography (SPCT) require materials with improved sensitivity.[70] The light yield per absorbed photon should be as high as possible, and the host lattice or its coating must be resistant towards radiation to avoid disturbing defect luminescence induced by radiation, as found for α-quartz.[71] Moreover, the reaction times have to be very short, because these limit the time resolution of the detector. The emission of the scintillator should be as homogeneous as possible to ensure a reliable integration of the data. There is still a great interest in better X-ray detection materials to enable X-ray investigations with lower radiation doses and faster evaluation.[72]

The relaxation times of conventional scintillation materials are too long; $CsI:Tl^+$, for example, exhibits a relaxation time of 800 ns. Therefore, suitable ions are sought which show allowed transitions during the detection process. The most promising activator ion is Ce^{3+}. If the Ce^{3+} ion is surrounded exclusively by oxygen or fluorine atoms, the 5d transitions are located so high on the energy scale that they can be excited directly from the 4f ground state. These transitions are allowed with respect to parity and spin selection rules and therefore are efficient and fast. The relaxation times that can be achieved for Ce^{3+} are in the range of 30 ns. The application of other trivalent rare-earth ions fails because of the formation of stable excitons[73] (as in $Lu_2Si_2O_7:Pr^{3+}$) or because numerous f states enable radiationless $5d \rightarrow 4f$ transitions (as in $Lu_2Si_2O_7:Nd^{3+}$).[74] The emission after excitation to d states of the respective $d \rightarrow f$ transition in $YPO_4:Nd^{3+}$ and $LuPO_4:Nd^{3+}$ peaks at 189 nm in the VUV and relaxes quite quickly.[75] Excitation into the conduction band, however, increases the decay time significantly.

Interesting candidates of current research are the Ce^{3+}-doped lutetium pyrosilicate $Lu_2Si_2O_7$[74] or the Ce^{3+}-doped bromine elpasolites $Cs_2NaLnBr_6$ (Ln = La, Y, Lu).[76] In principal the lanthanum halides should be very well suited owing to the relative hardness of the host lattices. Indeed, excellent light yields of up to 61 000 photons MeV^{-1} are found for $LaBr_3:Ce^{3+}$.[77] On the one hand, defects make LaF_3 (2200 photons MeV^{-1}) poorly suited as a scintillation material.[78] On the other hand, it seems more important that the 4f ground state of Ce^{3+} in LaF_3 lies energetically too high relative to the valence band, thus leading to an easy formation of stable excitons. Accordingly, the scintillation properties are enhanced in $LaCl_3$ (49 000 photons MeV^{-1}),[79,80] in which the valence band is located at higher energy, and they achieve best values for $LaBr_3$. LaI_3 exhibits the smallest band gap of the lanthanum halides and is a good scintillator below 200 K, with 16 000 photons MeV^{-1}. Above 200 K, rapid thermal quenching is observed. Apparently, in LaI_3 the lowest 5d states of Ce^{3+} are situated slightly below the conduction band. Thus, at low temperature an optimal energy transfer from the conduction band to the excited 5d state and subsequent fast emission is possible. Higher temperatures favor the thermal excitation from the 5d state to the conduction band and subsequent radiationless relaxation.[81] In contrast to $LaI_3:Ce^{3+}$, the Ce^{3+}-doped lutetium iodide $LuI_3:Ce^{3+}$ is a very good scintillator[82] with a decay time of 31 ns and a good light yield of 50 000 photons MeV^{-1}. Similarly doped $LuBr_3$ and $LuCl_3$ are found to be only slightly less efficient.[83]

$Cs_2LiYCl_6:Ce^{3+}$ is another very efficient neutron and γ-ray scintillator with a light yield of 70 000 photons per neutron.[84] The line shape of the Ce^{3+} emission changes with the excitation type (neutrons vs. γ-rays) and enables their distinction. For the elpasolites $Cs_2LiYCl_6:Ce^{3+}$ and $Cs_2LuCl_6:Ce^{3+}$[85] as well as for $LaI_3:Ce^{3+}$ at temperatures below 250 K, an anomalous cerium emission peaking at approximately 270 nm was observed, which could be elucidated recently.[86] The octahedral crystal-field splitting of the d states of Ce^{3+} in $Cs_2LiYCl_6:Ce^{3+}$ gives $5d_e$ und $5d_t$ terms. If excited, these states undergo Jahn–Teller distortion leading to a quite large energetic width. The anomalous Ce^{3+} emission can only be observed after direct excitation to the $5d_e$ states. Apparently, these are located in the conduction band and therefore allow strong interactions with excited states of the host material. The transitions are highly efficient and are classified as partial charge-transfer transitions with a decay time of 10 ns. At higher temperature, the excited electrons relax radiationlessly to the lower $5d_t$ levels and contribute to the normal cerium emission (Figure 4). Thus, these scintillators might be suitable below 250 K as specific detectors for UV radiation in the range of 200 to 220 nm.[86]

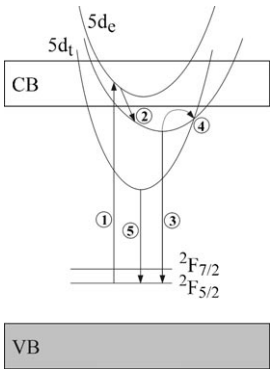

Figure 4. Energy-level scheme for the illustration of the anomalous Ce^{3+} emission (adapted from reference [86]; CB = conduction band, VB = valence band). After excitation from the $^2F_{5/2}$ ground state to a $5d_e$ level within the conduction band (1), a radiationless transition to a further $5d_e$ state occurs (2); there is then either the anomalous emission (3) or a radiationless transition (4) with subsequent normal emission from the $5d_t$ levels (5).

5. Nanostructured Phosphors

Although surface defects and lower crystallinity decrease the quantum efficiency of phosphor nanoparticles compared to conventionally sized phosphor particles, the nanoparticles offer opportunities for special applications, such as fluorescence markers.[87,88] Because of their small size, nanoparticles

do not scatter light and can be embedded very well in transparent materials such as glasses or plastic films. Luminescent transparent coatings could be made by simple printing methods.

The synthesis of monodisperse nanoparticles is a big challenge. Nanoparticles of conventional host lattice materials such as Y_2O_3, $LaPO_4$, $Sr_5(PO_4)_3Cl$, YVO_4, Zn_2SiO_4, and ZnS can be obtained by polyol-mediated syntheses.[89] With this advance, it also became possible to make accordingly doped phosphors $ZnS:Ag^+,Cl^-$, $LaPO_4:Ce^{3+},Tb^{3+}$, and $Y_2O_3:Eu^{3+}$ as nanoparticles.[90] An alternative approach is the preparation of such particles in ionic liquids under microwave irradiation.[91] The synthesis is quick and relatively simple. Moreover, the defect concentration is very low if the synthesis is carried out below 100 °C, and the particles are quite crystalline. These properties lead to comparably high quantum yields.[16,92] Doped nanoparticles of $LaPO_4:Eu^{3+}$ and $LaPO_4:Ce^{3+},Tb^{3+}$ prepared in this way can be used without further coating treatment by dispersion in an ethanol/methanol mixture. These nanoparticles can then be printed onto the desired substrate using an inkjet printer.[93] To remove structural defects, the particles can be tempered at 650 °C without change of their size. The emission spectra of the nanoscale phosphor particles are almost the same as those of the corresponding macroscale phosphor powders (Figure 5). Another advantage of these nanoparticles is that they are less hazardous than fluorescing CdTe or CdS nanoparticles and quantum dots.

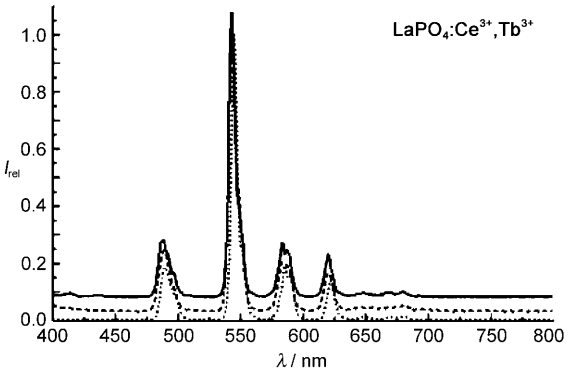

Figure 5. Emission spectra of $LaPO_4$:Ce,Tb under UV illumination (254 nm); as-prepared nanoparticles (-----) and nanoparticles tempered for 30 min at 650 °C (——) compared with the macroscale phosphor (•••••; illustration adapted from reference [93]).

6. Quantum-Cutting Phosphors

6.1. Gas Discharge Lamps

For environmental reasons, it is desirable to replace mercury-containing luminescent tubes with other light sources. Besides white-light-emitting diodes (Section 2), noble-gas-filled luminescent tubes might be an alternative. In contrast to other plasma light sources such as barium,[94,95] Mo/Ar,[96] or noble gases with added chlorine, such as Xe/Cl_2,[97] the noble gas plasma hardly reacts with the tube wall and the electrodes.[98]

The emissions in Xe vapor lamps are found around 147 (base line) and 172 nm (excimer band). The main emission in mercury vapor lamps is at 254 nm. In principal, many phosphors conventionally used in mercury plasma tubes might be also used in Xe plasma tubes. The main drawback of this approach is the lower efficiency resulting from the excitation of the conventional phosphors with higher energies, which reduces the energy efficiency from 60 (Hg plasma lamp) to 46 % (Xe plasma lamp). Furthermore, the significantly shorter emission wavelength places great demands on the stability of the phosphors towards radiation. The poor radiation stability of the classical phosphor BAM was already mentioned in Section 3.

6.2. Quantum Cutting

Radiation-resistant quantum-cutting phosphors might overcome this efficiency loss. They are capable of emitting more than one visible photon after absorption of a single high-energy photon. Thus, quantum efficiencies far above 100 % are expected. Preconditions for this process are high transition probabilities of the optical transitions and suitably positioned intermediate states with long lifetimes. The principle of quantum cutting has been known since the 1960s[99–102] and has moved back into the research focus in recent years. Trivalent rare-earth ions serve as activator ions. Quantum cutting works by making use of host-lattice states, by excitation of single ions (doped into a host lattice), and by excitation of ion pairs.[103]

The first demonstration of a quantum-cutting process was presented for samples of YF_3 and α-$NaYF_4$ doped with Pr^{3+}. The absorption of a high-energy photon yielded the emission of several photons.[99,104] These cascade emissions of Pr^{3+} can only be observed if the 4f5d levels are situated above the $^1S_0$ state of Pr^{3+}, as found in $CaMgAl_{14}O_{23}$ or LaF_3 (Figure 6). In this case, the Xe emission at 172 nm (58000 cm^{-1}) is absorbed by a parity-allowed and spin-allowed 4f→5d transition. The Pr^{3+} ion subsequently undergoes radiationless relaxation to

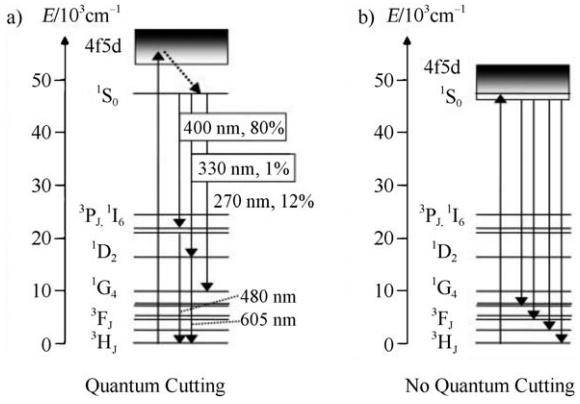

Figure 6. Illustration of the quantum-cutting process in Pr^{3+}-doped compounds[107] (left); if the 4f5d levels are too low energetically, no quantum cutting can be observed (right).

the rather stable $^1S_0$ state. From there, several emissions in the visible region are possible. If the energetic sequence of $^1S_0$ and d levels is changed, as in YBO_3 or YPO_4, only a broad-band emission assigned to 5d→4f transitions can be observed in the UV region.[105] Very careful investigations confirmed this fact in the series of complex fluorides K_2YF_5, $LiKYF_5$, KYF_4 doped with Pr^{3+}. Their emission spectra are dominated by the 5d→4f transition, while for CsY_2F_7 4f→4f transitions can be detected along with the 5d→4f fluorescence.[106] A similar situation is found in Cs_2KYF_6:Pr^{3+}, in which the Pr^{3+} ions are situated on yttrium and cesium sites. Careful spectroscopy showed that only the Pr^{3+} ions located on the cesium sites fulfill the preconditions for successful quantum cutting. The 5d levels lie above the $^1S_0$ state in this case.[99,104,107]

Apart from fluorides, oxide compounds could also be used as quantum cutters. Barium and strontium sulfate were doped with Pr^{3+}; the products emit blue (406 nm) and red light (600 nm) simultaneously after absorption into d levels.[108] In the case of $CaSO_4$, the d states again lie too low on the energetic scale. The desired cascade emission was also observed for $LaMgB_5O_{10}$:Pr^{3+}.[109] Unfortunately, the intensities of all compounds doped with Pr^{3+} are too low to achieve quantum efficiencies beyond 100%.

Quantum cutting can also be observed on ion pairs. A very well-investigated example is $LiGdF_4$ doped with Eu^{3+}.[110] Gd^{3+} acts as an absorber of a high-energy photon, which should emit up to two photons in cascade emission in Eu^{3+}. The basic drawback of Gd^{3+} as an absorber ion lies in the low transition probability of the participating parity-forbidden f→f transitions. Moreover, the host lattice takes part of the excitation energy, which is lost to radiationless relaxation.[111] Furthermore, oxygen contamination must be minimized to avoid charge-transfer transitions from Eu^{3+} to Eu^{2+}.

As mentioned above, parity-allowed 4f→5d transitions are better, because they show high transition probabilities. In $LiGdF_4$ doped with Er^{3+} and Tb^{3+}, the Er^{3+} ions can absorb the excitation energy by a parity-allowed f→d transition. A part of the energy is transferred via the Gd ions onto the green-emitting Tb^{3+} ions, while another part can be emitted in the green by relaxing the Er^{3+} ions. For this process a maximum quantum yield of 135% could be achieved.[112] This process needs an excitation energy of at least 6 eV: 2 eV are allotted to the Er emission, and further 4 eV are needed for the energy transfer via Gd onto Tb.[103] This phosphor might at first glance seem suited for use in conventional mercury plasma tubes, but the excitation energy of 4.9 eV (254 nm) is not sufficient.

In summary, progress has been made in the understanding of quantum-cutting phosphors, but a real breakthrough in terms of a phosphor that is efficient and stable towards hydrolysis and radiation has not yet been achieved.

7. Upconversion Phosphors in Solar Cells and Displays

Quantum cutters (Section 6) make use of the ability of trivalent rare-earth ions to convert one high-energy photon into several low-energy photons. The concept of upconversion has the opposite aim: to convert several low-energy photons into one high-energy photon. Important applications of such upconversion or anti-Stokes phosphors are the development of more efficient solar cells and transparent displays.

7.1. Solar Cells

Solar cells convert the electromagnetic radiation emitted by the sun into electric energy by semiconductor transitions. The lower border of usable sun energy is defined by the band gap of the semiconductor. In the case of silicon, this border is 1.1 eV, corresponding to a wavelength of 1.1 μm. Light of longer wavelength cannot be converted directly into electricity, although it contributes significantly to the total amount of emitted solar energy (Figure 7[113]). To make use of this part

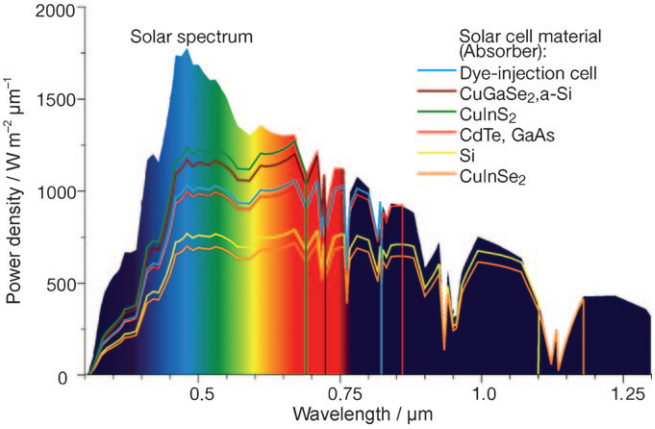

Figure 7. Solar emission spectrum as observed on the surface of the earth; the absorption lines of important semiconductors for use in solar cells are indicated.[113]

of the sunlight, phosphors are needed that are capable of converting such low-energy photons into short-wavelength light, so-called upconversion phosphors.

The solar cell is fitted with a layer that contains the upconversion phosphor (Figure 8). The silver mirror at the bottom reflects all the light which is not absorbed by the semiconductor layer. It thus passes the upconversion layer

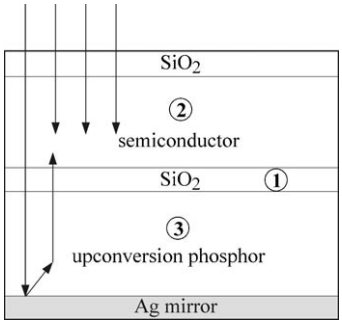

Figure 8. Principle of a solar cell; incident sunlight passes the semiconductor solar cell (2) coated with SiO_2 (1) and the layer containing the upconversion phosphor (3) before being reflected on a silver mirror (illustration adapted from reference [126]).

twice. There, a part of the long-wavelength light is converted into short-wavelength light. The incident sunlight is used more efficiently. By applying upconversion processes, it will be possible to generate electricity even in the dark (using IR radiation).

7.2. Upconversion Phosphors

The principle of upconversion phosphors was discovered as early as forty years ago.[114,115] As long as efficient excitation sources in the infrared spectral range were not available, upconversion did not play an important role. Moreover, the efficiency of the first examples was low. This situation changed when it was discovered that energy can be transferred much more efficiently using codoped phosphors. In 1966, Auzel showed on $CaWO_4$:Yb^{3+},Er^{3+}[116] and Woodward et al. on erbium-doped sodium silicate glasses the advantages of codoping for upconversion processes for the first time.[117] Er^{3+} is suitable as an activator ion because it has several almost equidistant energy levels (Figure 9). Er^{3+}-doped

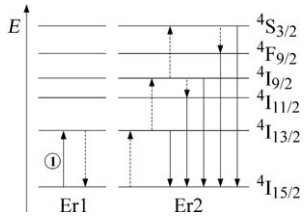

Figure 9. Upconversion process between two Er^{3+} ions; after excitation of an Er^{3+} ion (Er1) with 1520 nm (1), its relaxation may lead to a multiple energy transfer onto a second Er^{3+} ion (Er2), which subsequently emits light of shorter wavelength; dashed lines represent radiationless transitions (illustration adapted from reference [125]).

glasses have long been used as amplifier units in fiber optic cables for telecommunications.[118] Successfully tested emitter ions besides Er^{3+} are Yb^{3+}, Tm^{3+}, or Ho^{3+} in fluorides, oxide halides,[119–123] and chalcogenide glasses such as Ga_2S_3-La_2O_3.[124] Current investigations are focused on Er^{3+}-doped compounds such as $NaYF_4$:Er^{3+},[88,125] for which quantum efficiencies of around 6% were determined.[126] This is a rather good value for such upconversion processes.

7.3. Displays

In the course of the SHEDS program (SHEDS = super-high-efficiency diode sources), the first highly efficient infrared laser diodes were manufactured in 2005.[127] These were initially developed for the telecommunications industry for Er^{3+}-based amplifiers,[128] but these diodes, which have an optimized emission peak at 980 nm, also enable the excitation of Yb^{3+}. The upconversion mechanisms are shown in Figure 10. KY_3F_{10} codoped with 0.4% Tm^{3+} and 20% Yb^{3+} emits blue light under infrared excitation. After excitation of the

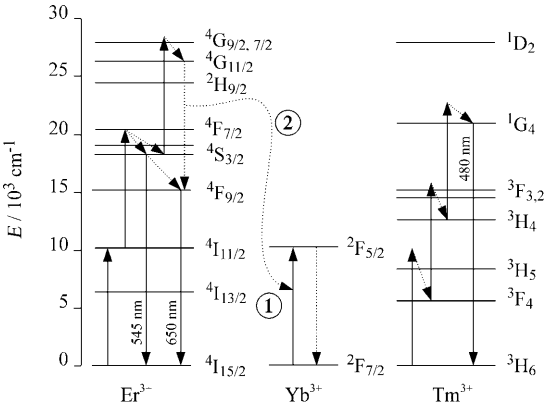

Figure 10. Upconversion mechanism in codoped Yb^{3+}/Er^{3+} and Yb^{3+}/Tm^{3+} compounds, respectively; Yb^{3+} is excited by infrared light (1) and transfers its energy onto an Er^{3+} ion, which then emits green or red light. Alternatively, the Yb^{3+} ion transfers its energy onto a Tm^{3+} ion, which emits blue light (illustration adapted from reference [129]).

$^2F_{7/2}\rightarrow{}^2F_{5/2}$ transition in Yb^{3+} by an infrared diode with an emission at 1 μm, the energy is transferred onto the coactivated Tm^{3+} ions. Afterwards, these show a blue emission at 480 nm ($^1G_4\rightarrow{}^3H_6$).

In the case of codoping Yb^{3+} with Er^{3+}, either the luminescence of the transition $^4S_{3/2}\rightarrow{}^4I_{15/2}$ at 545 nm (green) or of the transition $^4F_{9/2}\rightarrow{}^4I_{15/2}$ at 650 nm (red) dominates, depending on the host lattice. The undesired second emission is filtered. A certain admixture of the respective other color may give better color-rendering indices during operation of displays. YF_3 codoped with 18% Yb^{3+} and 1% Er^{3+} emits red light, and $NaYF_4$ doped in the same manner favors the green emission.[129] After radiationless relaxation of the $^4S_{3/2}$ state it can also emit red. The absorption of a third infrared photon from the $^4S_{3/2}$ state and an energy transfer (2) back to Yb^{3+} is another alternative, as shown in Figure 10.[130]

In principle these upconversion phosphors are suited for the application in transparent displays in which the pixels are excited by infrared laser diodes. The quantum efficiency of such phosphors achieves values of 4% in the case of KY_3F_{10}:Yb^{3+},Tm^{3+} and up to 8% in YF_3:Yb^{3+},Er^{3+}.[129] Owing to the excitation time of approximately half a millisecond and the decay time of approximately two milliseconds, these phosphors are apparently suited for the application in displays.

8. Summary and Outlook

Great progress has been achieved in the area of new scintillator materials, and scintillation mechanisms could be elucidated. Nevertheless, research is still active, and the need for more efficient and more quickly relaxing materials is still given. During the last ten years, the development of white-light-emitting diodes made a large step forward, but the story continues, especially for white LEDs based on diodes emitting in the UV region. Moreover, the fine adjustment of diode emission and the excitation spectra of the phosphors has the potential to further increase efficiency. Almost no progress

was achieved in the area of new quantum-cutter phosphors. The intensity of research interest in this field lets us hope for a real breakthrough in the long term. Upconversion phosphors are of increasing interest for applications in the coating of solar cells and in displays. Promising candidates have already been identified, but more research is needed. New host-lattice classes like the nitridosilicates[17] and thiosilicates[42] as well as the rediscovery of older solid-state compounds such as phosphates as host lattices[38] deliver new impulses for a further increase of phosphor efficiency up to the borders of the physically possible.

Received: August 13, 2008
Published online: April 6, 2009

[1] T. Jüstel, H. Nikol, C. Ronda, *Angew. Chem.* **1998**, *110*, 3250; *Angew. Chem. Int. Ed.* **1998**, *37*, 3084.
[2] G. F. de Sá, O. L. Malta, C. de Mello Donegá, A. M. Simas, R. L. Longo, P. A. Santa-Cruz, E. F. da Silva, Jr., *Coord. Chem. Rev.* **2000**, *196*, 165.
[3] F. So, B. Krummacher, M. K. Mathai, D. Poplavskyy, S. A. Choulis, V.-E. Choong, *J. Appl. Phys.* **2007**, *102*, 091101.
[4] F. Goubin, X. Rocquefelte, M.-H. Whangbo, Y. Montanardi, R. Brec, S. Jobic, *Chem. Mater.* **2004**, *16*, 662.
[5] The quantum efficiency is equal to the ratio of emitted to absorbed photons.
[6] P. Dorenbos, *J. Phys. Condens. Matter* **2003**, *15*, 575.
[7] P. Dorenbos, *J. Lumin.* **2005**, *111*, 89.
[8] G. H. Dieke, *Spectra and Energy Levels of Rare Earth Ions in Crystals*, Wiley Interscience, New York, **1968**.
[9] W. T. Carnall, G. L. Goodman, K. Rajnak, R. S. Rana, *A systematic analysis of the spectra of lanthanides doped into single crystal LaF_3*, ANL-88–8, Argonne, **1988**, p. 70.
[10] R. T. Wegh, A. Meijerink, R.-J. Lamminmäki, J. Hölsä, *J. Lumin.* **2000**, *87–89*, 1002.
[11] S. Nakamura, T. Mukai, M. Senoh, *Appl. Phys. Lett.* **1994**, *64*, 1687.
[12] M. Born, T. Jüstel, *Phys. J.* **2003**, *2*, 43.
[13] U. Kaufmann, M. Kunzer, K. Köhler, H. Obloh, W. Pleschen, P. Schlotter, J. Wagner, A. Ellens, W. Rossner, M. Kobusch, *Phys. Status Solidi A* **2002**, *192*, 246.
[14] S. Nakamura, G. Fasol, *The Blue Laser Diode*, Springer, Berlin **1997**.
[15] The color temperature of a radiator is equal to the temperature for which its emission is equivalent to the color of a black-body radiator at that temperature; thus, bluish-white light exhibits a high color temperature, while warm-white light corresponds to a low color temperature.
[16] C. Feldmann, T. Jüstel, C. R. Ronda, P. J. Schmidt, *Adv. Funct. Mater.* **2003**, *13*, 511.
[17] R. Mueller-Mach, G. Mueller, M. R. Krames, H. A. Höppe, F. Stadler, W. Schnick, T. Jüstel, P. Schmidt, *Phys. Status Solidi A* **2005**, *202*, 1727.
[18] R.-J. Xie, N. Hirosaki, *Sci. Technol. Adv. Mater.* **2007**, *8*, 588.
[19] H. A. Höppe, H. Lutz, P. Morys, W. Schnick, A. Seilmeier, *J. Phys. Chem. Solids* **2000**, *61*, 2001.
[20] H. A. Höppe, F. Stadler, O. Oeckler, W. Schnick, *Angew. Chem.* **2004**, *116*, 5656; *Angew. Chem. Int. Ed.* **2004**, *43*, 5540.
[21] F. Stadler, O. Oeckler, H. A. Höppe, M. H. Möller, R. Pöttgen, B. D. Mosel, P. Schmidt, V. Duppel, A. Simon, W. Schnick, *Chem. Eur. J.* **2006**, *12*, 6984.
[22] Y. Q. Li, G. de With, H. T. Hintzen, *J. Solid State Chem.* **2008**, *181*, 515.
[23] C.-C. Yang, C.-M. Lin, Y.-J. Chen, Y.-T. Wu, S.-R. Chuang, R.-S. Liu, S.-F. Hu, *Appl. Phys. Lett.* **2007**, *90*, 123503.
[24] K. Uheda, H. Takizawa, T. Endo, H. Yamane, M. Shimada, C.-M. Wang, M. Mitomo, *J. Lumin.* **2000**, *87–89*, 967.
[25] H. Kamioka, T. Yamaguchi, M. Hirano, T. Kamiya, H. Hosono, *J. Lumin.* **2007**, *122/123*, 339.
[26] U. Kaufmann, M. Kunzer, K. Köhler, H. Obloh, W. Pletschen, P. Schlotter, J. Wagner, A. Ellens, W. Rossner, M. Kobusch, *Phys. Status Solidi A* **2002**, *192*, 246.
[27] M. R. Davolos, A. Garcia, C. Fouassier, P. Hagenmuller, *J. Solid State Chem.* **1989**, *83*, 316.
[28] T. E. Peters, J. A. Baglio, *J. Electrochem. Soc.* **1972**, *119*, 230.
[29] C. Chartier, P. Benalloul, C. Barthou, J.-M. Frigerio, G. O. Mueller, R. Mueller-Mach, T. Trottier, *J. Phys. D* **2002**, *35*, 363.
[30] R. Eholie, M. O. Gorochov, M. Guittard, M. A. Mazurier, M. J. Flahaut, *Bull. Soc. Chim. Fr.* **1971**, 747.
[31] T. Baby, V. P. N. Nampoori, *Solid State Commun.* **1988**, *68*, 821.
[32] C. Wickleder, S. Zhang, H. Haeuseler, *Z. Kristallogr.* **2005**, *220*, 277.
[33] A. Nag, P. J. Schmidt, W. Schnick, *Chem. Mater.* **2006**, *18*, 5738.
[34] C. Wickleder, *Chem. Mater.* **2005**, *17*, 1228.
[35] C. Wickleder, *J. Alloys Compd.* **2004**, *374*, 10.
[36] A. Sandhu, *Nat. Photonics* **2007**, *1*, 37.
[37] H. A. Höppe, M. Daub, M. C. Bröhmer, *Chem. Mater.* **2007**, *19*, 6358.
[38] H. A. Höppe, *Solid State Sci.* **2005**, *7*, 1209.
[39] J. O. Rubio, A. F. Muñoz, C. Zaldo, H. S. Murrieta, *Solid State Commun.* **1988**, *65*, 251.
[40] W.-J. Yang, L. Luo, T.-M. Chen, N.-S. Wang, *Chem. Mater.* **2005**, *17*, 3883.
[41] J. S. Kim, Y. H. Park, J. C. Choi, H. L. Park, *Electrochem. Solid-State Lett.* **2005**, *8*, H65.
[42] P. F. Smet, K. Korthout, J. E. van Haecke, D. Poelman, *Mater. Sci. Eng. B* **2008**, *146*, 264.
[43] Vacuum UV radiation refers to the wavelength range below 200 nm, which is absorbed almost completely by air.
[44] S. Zhang, *IEEE Trans. Plasma Sci.* **2006**, *34*, 294.
[45] D. Gourier, T. Gbehi, R. Visocekas, J. Thery, D. Vivien, *Phys. Status Solidi B* **1989**, *152*, 415.
[46] Z. Wu, A. N. Cormack, *J. Electroceram.* **2003**, *10*, 179.
[47] T. Jüstel, H. Bechtel, W. Mayr, D. U. Wiechert, *J. Lumin.* **2003**, *104*, 137.
[48] V. Pike, S. Patraw, A. L. Diaz, B. G. DeBoer, *J. Solid State Chem.* **2003**, *173*, 359.
[49] S. Oshio, T. Matsuoka, S. Tanaka, H. Kobayashi, *J. Electrochem. Soc.* **1998**, *145*, 3903.
[50] S. Zhang, T. Kono, A. Ito, T. Yasaka, H. Uchiike, *J. Lumin.* **2004**, *106*, 39.
[51] S. H. M. Poort, W. P. Blokpoel, G. Blasse, *Chem. Mater.* **1995**, *7*, 1547.
[52] J. Zhang, Z. Zhang, Z. Tang, Y. Tao, X. Long, *Chem. Mater.* **2002**, *14*, 3005.
[53] R. P. Rao, *J. Lumin.* **2005**, *113*, 271.
[54] A. W. Veenis, A. Bril, *Philips J. Res.* **1978**, *33*, 124.
[55] Y. Wang, X. Guo, T. Endo, Y. Murakami, M. Ushirozawa, *J. Solid State Chem.* **2004**, *177*, 2242.
[56] Color purity is a standard value defined by the European Broadcasting Union (EBU). It determines the tolerances around ideal color points of the three basic colors to ensure a correct display of a broadcasted picture. The color coordinates of a phosphor have to be located within these tolerances to be suited for the application in a display.
[57] G. Blasse, B. C. Grabmeier, *Luminescent materials*, 1st ed., Springer, Berlin, **1994**.
[58] T. Hase, T. Kano, E. Nakazawa, H. Yamamoto, *Adv. Electron. Electron Phys.* **1990**, *79*, 271.

[59] K.-S. Sohn, C.-H. Kim, J.-T. Park, H.-D. Park, *J. Mater. Res.* **2002**, *17*, 3201.
[60] Z.-G. Wei, L.-D. Sun, C.-S. Liao, C.-H. Yan, S.-H. Huang, *Appl. Phys. Lett.* **2002**, *80*, 1447.
[61] Z. Yu, X. Huang, W. Zhuang, X. Cui, H. Li, *J. Alloys Compd.* **2005**, *390*, 220.
[62] C. Okazaki, M. Shiiki, T. Suzuki, K. Suzuki, *J. Lumin.* **2000**, *87–89*, 1280.
[63] E. van der Kolk, P. Dorenbos, C. W. E. van Eijk, H. Bechtel, T. Jüstel, H. Nikol, C. R. Ronda, D. U. Wiechert, *J. Lumin.* **2000**, *87–89*, 1246.
[64] Y. C. Kang, M. A. Lim, H. D. Park, M. Han, *J. Electrochem. Soc.* **2003**, *150*, H7.
[65] R. P. Rao, *J. Electrochem. Soc.* **2003**, *150*, H165.
[66] G. Blasse, B. C. Grabmeier, *Luminescent Materials*, Springer, Berlin, **1994**.
[67] M. Sonoda, M. Takano, J. Miyahara, H. Kato, *Radiology* **1983**, *148*, 833.
[68] C. T. Schmidt, *IRE Trans. Nucl. Sci.* **1960**, *7*, 25.
[69] G. F. J. Garlick, R. A. Fatehally, *Phys. Rev.* **1949**, *75*, 1446.
[70] C. W. E. van Eijk, *Nucl. Instrum. Methods Phys. Res. Sect. A* **1994**, *348*, 546.
[71] M. Cannas, S. Agnello, F. M. Gelardi, R. Boscaino, A. N. Trukhin, P. Liblik, C. Lushchik, M. F. Kink, Y. Maksimov, R. A. Kink, *J. Phys. Condens. Matter* **2004**, *16*, 7931.
[72] C. W. E. van Eijk, *Phys. Med. Biol.* **2002**, *47*, R85.
[73] Excitons are quasi-particles that consist of an excited electron and the respective hole.
[74] L. Pidol, B. Viana, A. Kahn-Harari, A. Bessiere, P. Dorenbos, *Nucl. Instrum. Methods Phys. Res. Sect. A* **2005**, *537*, 125.
[75] V. N. Makhov, N. Yu. Kirikova, M. Kirm, J. C. Krupa, P. Liblik, A. Lushchik, Ch. Lushchik, E. Negodin, G. Zimmerer, *Nucl. Instrum. Methods Phys. Res. Sect. A* **2002**, *486*, 437.
[76] M. D. Birowosuto, P. Dorenbos, C. W. E. van Eijk, K. W. Krämer, H. U. Güdel, *J. Phys. Condens. Matter* **2006**, *18*, 6133.
[77] E. V. D. van Loef, P. Dorenbos, C. W. E. van Eijk, K. W. Krämer, H. U. Güdel, *Appl. Phys. Lett.* **2001**, *79*, 1573.
[78] M. R. Levy, A. Patel, C. R. Stanek, K. McClellan, R. W. Grimes, *Phys. Status Solidi C* **2007**, *4*, 1226.
[79] O. Guillot-Noël, J. T. M. de Haas, P. Dorenbos, C. W. E. van Eijk, K. Krämer, H. U. Güdel, *J. Lumin.* **1999**, *85*, 21.
[80] E. V. D. van Loef, P. Dorenbos, C. W. E. van Eijk, K. Krämer, H. U. Güdel, *Appl. Phys. Lett.* **2000**, *77*, 1467.
[81] A. Bessiere, P. Dorenbos, C. W. E. van Eijk, K. W. Krämer, H. U. Güdel, C. de Mello Donega, A. Meijerink, *Nucl. Instrum. Methods Phys. Res. Sect. A* **2005**, *537*, 22.
[82] J. Glodo, K. S. Shah, M. Klugerman, P. Wong, B. Higgins, P. Dorenbos, *Nucl. Instrum. Methods Phys. Res. Sect. A* **2005**, *537*, 279.
[83] E. V. D. van Loef, P. Dorenbos, C. W. E. van Eijk, K. W. Krämer, H. U. Güdel, *Nucl. Instrum. Methods Phys. Res. Sect. A* **2003**, *496*, 138.
[84] A. Bessière, P. Dorenbos, C. W. E van Eijk, L. Pidol, K. W. Krämer, H. U. Güdel, *Nucl. Instrum. Methods Phys. Res. Sect. A* **2005**, *537*, 242.
[85] P. Dorenbos, E. V. D. van Loef, C. W. E. van Eijk, K. W. Krämer, H. U. Güdel, *Phys. Rev. B* **2003**, *68*, 125108.
[86] A. Bessière, P. Dorenbos, C. W. E van Eijk, L. Pidol, K. W. Krämer, H. U. Güdel, *J. Phys. Condens. Matter* **2004**, *16*, 1887.
[87] M. A. Aegerter, J. Puetz, G. Gasparro, N. Al-Dahoudi, *Opt. Mater.* **2004**, *26*, 155.
[88] J. F. Suyver, A. Aebischer, D. Biner, P. Gerner, J. Grimm, S. Heer, K. W. Krämer, C. Reinhard, H. U. Güdel, *Opt. Mater.* **2005**, *27*, 1111.
[89] C. Feldmann, *Solid State Sci.* **2005**, *7*, 868.
[90] C. Feldmann, *Adv. Funct. Mater.* **2003**, *13*, 101.
[91] G. Bühler, C. Feldmann, *Angew. Chem.* **2006**, *118*, 4982; *Angew. Chem. Int. Ed.* **2006**, *45*, 4864.
[92] S. Shionoya, W. M. Yen, *Phosphor Handbook*, CRC Press, Boca Raton **1999**.
[93] G. Bühler, C. Feldmann, *Appl. Phys. A* **2007**, *87*, 631.
[94] X. L. Peng, J. J. Curry, G. G. Lister, J. E. Lawler, *J. Appl. Phys.* **2002**, *91*, 1761.
[95] J. Laski, G. G. Lister, F. Palmer, P. E. Moskowitz, *J. Appl. Phys.* **2002**, *91*, 1772.
[96] J. L. Giuliani, G. M. Petrov, R. E. Pechacek, R. A. Meger, *IEEE Trans. Plasma Sci.* **2003**, *31*, 564.
[97] A. P. Golovitskii, *Tech. Phys. Lett.* **1998**, *24*, 233.
[98] D. Uhrlandt, R. Bussiahn, S. Gorchakov, H. Lange, D. Loffhagen, D. Nötzold, *J. Phys. D* **2005**, *38*, 3318.
[99] E. Ilmas, G. Liidja, Ch. B. Lushchik, *Opt. Spektrosk.* **1965**, *18*, 453.
[100] E. Ilmas, G. Liidja, C. B. Lushchik, *Opt. Spektrosk.* **1965**, *18*, 631.
[101] E. Ilmas, Ch. B. Lushchik, *Tr. Inst. Fiz. Astron., Akad. Nauk Est. SSR* **1966**, *34*, 5.
[102] J. L. Sommerdijk, A. Bril, A. W. de Jager, *J. Lumin.* **1974**, *8*, 341.
[103] C. Ronda, *J. Lumin.* **2002**, *100*, 301.
[104] W. W. Piper, J. A. de Luca, F. S. Ham, *J. Lumin.* **1974**, *8*, 344.
[105] F. You, S. Huang, C. Meng, D. Wang, J. Xu, Y. Huang, G. Zhang, *J. Lumin.* **2007**, *122–123*, 58.
[106] V. N. Makhov, N. M. Khaidukov, D. Lo, M. Kirm, G. Zimmerer, *J. Lumin.* **2003**, *102–103*, 638.
[107] D. Schiffbauer, C. Wickleder, G. Meyer, M. Kirm, M. Stephan, P. C. Schmidt, *Z. Anorg. Allg. Chem.* **2005**, *631*, 3046.
[108] E. van der Kolk, P. Dorenbos, A. P. Vink, R. C. Perego, C. W. E. van Eijk, A. R. Lakshmanan, *Phys. Rev. B* **2001**, *64*, 195129.
[109] A. M. Srivastava, D. A. Doughty, W. W. Beers, *J. Electrochem. Soc.* **1996**, *143*, 4113.
[110] R. T. Wegh, H. Donker, K. D. Oskam, A. Meijerink, *Science* **1999**, *283*, 663.
[111] C. Feldmann, T. Jüstel, C. R. Ronda, D. U. Wiechert, *J. Lumin.* **2001**, *92*, 245.
[112] K. D. Oskam, R. T. Wegh, H. Donker, E. V. D. van Loef, A. Meijerink, *J. Alloys Compd.* **2000**, *300–301*, 421.
[113] Helmholtz-Zentrum Berlin für Materialien und Energie GmbH (previously Hahn-Meitner-Institut).
[114] N. Bloembergen, *Phys. Rev. Lett.* **1959**, *2*, 84.
[115] L. Esterowitz, A. Schnitzler, J. Noonan, J. Bahler, *Appl. Opt.* **1968**, *7*, 2053.
[116] F. Auzel, *C. R. Seances Acad. Sci. Ser. C* **1966**, *262*, 1016.
[117] R. J. Woodward, J. M. Williams, M. R. Brown, *Phys. Lett.* **1966**, *22*, 435.
[118] F. Auzel, *Ann. Telecommun.* **1969**, *24*, 363.
[119] L. F. Johnson, J. E. Geusic, H. J. Guggenheim, T. Kushida, S. Singh, L. G. Van Uitert, *Appl. Phys. Lett.* **1969**, *15*, 48.
[120] H. J. Guggenheim, L. F. Johnson, *Appl. Phys. Lett.* **1969**, *15*, 51.
[121] L. G. Van Uitert, S. Singh, H. J. Levinstein, L. F. Johnson, W. H. Grodkiewicz, J. E. Geusic, *Appl. Phys. Lett.* **1969**, *15*, 53.
[122] J. E. Geusic, F. W. Ostermayer, H. M. Marcos, L. G. Van Uitert, J. P. van der Ziel, *J. Appl. Phys.* **1971**, *42*, 1958.
[123] L. Esterowitz, J. Noonan, J. Bahler, *Appl. Phys. Lett.* **1967**, *10*, 126.
[124] H. T. Amorim, M. T. de Araujo, E. A. Gouveia, A. S. Gouveia-Neto, J. A. Medeiros Neto, A. S. B. Sombra, *Opt. Mater.* **1998**, *10*, 241.
[125] A. Shalav, B. S. Richards, T. Trupke, K. W. Krämer, H. U. Güdel, *Appl. Phys. Lett.* **2005**, *86*, 013505.
[126] B. S. Richards, A. Shalav, *IEEE Trans. Electron Devices* **2007**, *54*, 2679.
[127] "SHEDS: The next revolution for the laser diode" in *Photon. Spectra* **2005**, 89.

[128] M. Fox, *Optical Properties of Solids*, Oxford University Press, Oxford, **2001**.
[129] A. Rapaport, J. Milliez, M. Bass, A. Cassanho, H. Jenssen, *J. Disp. Technol.* **2006**, *2*, 68.
[130] J. L. Sommerdijk, *J. Lumin.* **1971**, *4*, 441.
[131] T. Mukai, S. Nagahama, N. Iwasa, M. Senoh, T. Yamada, *J. Phys. Condens. Matter* **2001**, *13*, 7089–7098; M. R. Krames, O. B. Shchekin, R. Mueller-Mach, G. O. Mueller, L. Zhou, G. Harbers, M. G. Craford, *J. Disp. Technol.* **2007**, *3*, 160–175.

